Temperature Effect on Vibration Analysis of Annular Graphene Sheet Embedded on Visco-Pasternak Foundation

M. Mohammadi[1,*], A. Farajpour[2], M. Goodarzi[1], H. Mohammadi[3]

[1]*Department of Engineering, Ahvaz Branch, Islamic Azad University, Ahvaz, Iran*
[2]*Young Researches and Elites Club, North Tehran Branch, Islamic Azad University, Tehran, Iran*
[3]*Department of Electrical Engineering, Shahid Chamran University of Ahvaz, Iran*

ABSTRACT

In this study, the vibration behavior of circular and annular graphene sheet embedded in a Visco-Pasternak foundation and coupled with temperature change and under in-plane pre-load is studied. The single-layered annular graphene sheet is coupled by an enclosing viscoelastic medium which is simulated as a Visco- Pasternak foundation. By using the nonlocal elasticity theory and classical plate theory, the governing equation is derived for single-layered graphene sheets (SLGSs). The closed-form solution for frequency vibration of circular graphene sheets has been obtained and nonlocal parameter, in-plane pre-load, the parameters of elastic medium and temperature change appears into arguments of Bessel functions. To verify the accuracy of the present results, the new version differential quadrature method (DQM) is also developed. Closed-form results are successfully verified with those of the DQM results. The results are subsequently compared with valid result reported in the literature. The effects of the small scale, pre-load, mode number, temperature change, elastic medium and boundary conditions on natural frequencies are investigated. The non-dimensional frequency decreases at high temperature case with increasing the temperature change for all boundary conditions. The effect of temperature change on the non-dimensional frequency vibration becomes the opposite at high temperature case in compression with the low temperature case. The present research work thus reveals that the nonlocal parameter, boundary conditions, temperature change and initial pre-load have significant effects on vibration response of the circular nanoplates. The present analysis results can be used for the design of the next generation of nanodevices that make use of the thermal vibration properties of the graphene.

© 2013 IAU, Arak Branch. All rights reserved.

Keywords: Vibration ;Annular graphene sheet ;Temperature change ; In-plane pre-load

1   INTRODUCTION

IN the new epoch, the investigation of the behavior of matters at the atomic scale of material is the focus of international scientific community. The growth of scientists at this length scale has concentrating on creating the nanotechnology phrase. Nanotechnology is studied one of the most encouraging technologies to be researched now. This technology could have enormous influence on information technology, aerospace, electronic devices, defense production and medical devices. Many endeavors have been made to construct nanodevices, expand and utilize matters on the nano scale [1]. Some encouraging utilization has commenced to appear. one of the best samples of novel nanostructures are carbon nanotubes (CNTs). CNTs are allotropes of carbon. These are derived by bottom-up chemical synthesis processes. In CNTs, the chemical compound and atomic bonding configuration is simple. To use

graphene sheets properly as nano electro-mechanical system design and micro electro-mechanical systems (NEMS and MEMS) component, their frequency response with small-scale effects should be investigated.

Graphene is a truly two-dimensional atomic crystal with exceptional electronic and mechanical properties. Many nanostructures based on the carbon such as carbon nanotube [2], nanorings [3], etc. are considered as deformed graphene sheet. Hence, so analysis of graphene sheets is a basic matter in the study of the nanomaterials.

Continuum modeling of CNTs has also increasing deal of attention of many researchers due to the fact that experiments in nanoscale are difficult [4] and molecular dynamic simulations are highly computationally expensive. There are various size-dependent continuum theories such as couple stress theory [5], strain gradient elasticity theory [6], modified couple stress theory [7] and nonlocal elasticity theory [8]. Among these theories, nonlocal elasticity theory, introduced by Eringen in 1983 [8], has been widely applied [9-22]. He modified the classical continuum mechanics for taking into account small scale effects. In this theory, the stress state at a given point depends on the strain states at all points, while in the local theory, the stress state at any given point depends only on the strain state at that point. As we have mentioned above, the mechanical behaviours of CNTs are investigated by many researchers. Mohammadi et al. [23] studied vibration of orthotropic rectangular graphene sheet under biaxial in-plane pre-load. They reported that Numerical results are presented using the nonlocal theories to bring out the effect of the nonlocal behavior on natural frequencies of rectangular SLGSs. Ke et al. [24] studied axisymmetric nonlinear free vibration of size-dependent functionally graded (FG) annular microplates. They considered that unlike homogeneous microplates, the FG material microplates display different vibration behavior at positive and negative amplitudes due to the presence of bending-extension coupling. A dynamical behavior of circular and annular FG material was studied using Reddy's plate theory [25]. Mohammadi et al. [26] investigated the buckling of rectangular SLGSs under shear in-plane load and in thermal environment. They showed that the critical shear buckling load of rectangular SLGSs is strongly dependent on the small scale coefficient. Civalek and Akgoz [27] analyzed the vibration behavior of micro-scaled sector shaped graphene surrounded by an elastic matrix. Murmu and Pradhan [28] employed the nonlocal elasticity theory for the vibration analysis of rectangular SLGSs embedded in an elastic medium. They have used both Winkler-type and Pasternak-type models for simulate the interaction of the graphene sheets with a surrounding elastic medium. They reported that the natural frequencies of SLGSs are strongly dependent on the small scale coefficients. Pradhan and Phadikar [29] investigated the vibration of embedded multilayered graphene sheets (MLGS) based on nonlocal continuum models. In their paper, they have shown that nonlocal effect is quite significant and needs to be included in the continuum model of graphene sheet. Yi-Ze Wang et al. [30] studied the vibration of double-layered nanoplate. In their research, thermal effect and nanoplate with isotropic mechanical properties was shown. It has been reported that graphene sheets have orthotropic properties [31]. Aksencer and Aydogdu [32] proposed levy type solution for vibration and buckling of nanoplate. In that paper, they considered rectangular nanoplate with isotropic property and without effect of elastic medium. Malekzadeh et al. [33] used the differential quadrature method (DQM) to study the thermal buckling of a quadrilateral nanoplates embedded in an elastic medium. Thermal vibration analysis of orthotropic nanoplates based on nonlocal continuum mechanics were studied by Satish et al. [34] who considerate two variable refined plate theory for thermal vibration of orthotropic nanoplate. In general, SLGSs are embedded in an elastic medium but they didn't consider effect of elastic medium in that paper. On the other hand, they represented vibration frequency of rectangular nanoplate only for simply supported boundary conditions and they didn't represent vibration frequency for other boundary conditions. Prasanna Kumar et al. [35] represented thermal vibration analysis of monolayer graphene sheet embedded in an elastic medium via nonlocal continuum theory. In their paper, they considered simply support boundary condition and they didn't study other boundary condition. They investigated graphene sheet with isotropic property. Farajpour et al. [36] studied axisymmetric buckling of the circular graphene sheets with the nonlocal continuum plate model. In that paper, the buckling behavior of circular nanoplates under uniform radial compression is studied. Explicit expressions for the buckling loads are obtained for clamped and simply supported boundary conditions. It is shown that nonlocal effects play an important role in the buckling of circular nanoplates. In that paper, their results compared with the results obtained by molecular dynamic and it is observed that results predicted by nonlocal theory are in exact match with MD results. Thus the reliability of nonlocal theory and presented solution is demonstrated. Mohammadi et al [37] employed the nonlocal plate theory to analyze vibration of circular and annular graphene sheet. They founded that scale effect is less prominent in lower vibration mode numbers and is highly prominent in higher mode numbers.

It is cleared that the natural frequency is easily affected by the applied temperature change. As a result, the effect of temperature change on the property of transverse vibration of graphene sheet is of practical interest. Thermal expansion is the tendency of matter to change in volume in response to a change in temperature [38]. When a substance is heated; its particles begin moving more and thus usually maintain a greater average separation.

Materials which contract with increasing temperature are unusual; this effect is limited in size and only occurs within limited temperature ranges. The degree of expansion divided by the change in temperature is called the material's coefficient of thermal expansion and generally varies with temperature. A number of materials contract on heating within certain temperature ranges; this is usually called negative thermal expansion, rather than "thermal contraction". For example, the coefficient of thermal expansion of water drops to zero as it is cooled to 3.983 °C and then becomes negative below this temperature; this means that water has a maximum density at this temperature, and this leads to bodies of water maintaining this temperature at their lower depths during extended periods of sub-zero weather. Fairly pure silicon has a negative coefficient of thermal expansion for temperatures between about 18 and 120 Kelvin [39]. Jiang et al. [40] investigated thermal expansion for single wall carbon nanotubes (SWCNTs). They developed an analytical method to determine the coefficient of thermal expansion for SWCNTs in radial and axial directions with interatomic potential and the local harmonic model. They founded that all coefficient thermal expansions are negative at low and room temperature and become positive at high temperature. Alamusi et al. [41] predicted the thermal expansion properties of carbon nanotube with molecular dynamics simulation. They reported that within a wide low temperature range, axial coefficient thermal expansions of SWCNTs are negative. As the diameter of CNTs decreases, this temperature range for negative axial coefficient thermal expansions becomes narrow, and positive axial coefficient thermal expansions appear in high temperature range. Yao and Han [42] studied the buckling analysis of multi-walled carbon nanotubes (MWCNTs) under torsional load coupling and temperature change. They reported that the CNTs have a positive coefficient of thermal expansion for temperature above 200 Kelvin.

It is clear that the natural frequency is easily affected by the applied in-plane pre-load and temperature change. As a result, the effect of in-plane pre-load on the property of transverse vibration of graphene sheet is of practical interest. Researches that investigated on the nonlocal annular graphene sheets are very limited in number with respect to the case of rectangular nanoplate. To the best knowledge of authors, it is the first time the nonlocal elasticity theory has been successfully applied to investigate the vibration frequency of annular graphene sheets embedded in a Visco-Pasternak elastic medium under thermal environment. The influence of the surrounding elastic medium on the frequency vibration of the annular SLGSs is investigated. In the present paper, the effect of the in-plane pre-load and temperature change on the vibration frequency of single layered annular graphene sheet is investigated. The governing equation of motion is derived using the nonlocal elasticity theory. Exact solution for the frequency equations of annular nanoplate with simply supported, clamped boundary conditions and mix of them are derived and nonlocal parameter, in-plane pre load and temperature change appears into arguments of Bessel functions. From the results, some new and absorbing phenomena can be observed. To suitably design nano electro-mechanical system and micro electro-mechanical systems (NEMS/MEMS) devices using graphene sheets, the present results would be useful.

2   DIFFERENTIAL EQUATIONS FOR NANOPLATES

The governing differential equation for vibration analysis nanoplate surrounded by Visco-Pasternak foundation is [43]

$$\frac{\partial^2 M_{xx}}{\partial x^2} + 2\frac{\partial^2 M_{xy}}{\partial x \partial y} + \frac{\partial^2 M_{yy}}{\partial y^2} + f + \frac{\partial}{\partial x}\left(N_{xx}\frac{\partial w}{\partial x} + N_{xy}\frac{\partial w}{\partial y}\right) + \frac{\partial}{\partial y}\left(N_{yy}\frac{\partial w}{\partial y} + N_{xy}\frac{\partial w}{\partial x}\right)$$
$$= \rho h \frac{\partial^2 w}{\partial t^2} + K_w w - K_G \nabla^2 w + C_d \frac{\partial w}{\partial t}$$

(1)

Here, f, ρ, C_d, K_w, K_G are distributed transverse load acting on the nanoplate per unit area of the nanoplate, density, Damper modulus parameters, Winkler modulus and the shear modulus of the surrounding elastic medium, respectively. The dimensions of Winkler modulus, Shear modulus of the surrounding elastic medium and damper

modulus are N/m^3, N/m and $N.s/m^2$ respectively [44, 45]. It is assumed that the nanoplate is free from any transverse loadings ($f = 0$). The terms M_{xx}, M_{xy}, M_{yy} are stress resultants that they are defined as [35]

$$M_{xx} - (e_0 l_i)^2 \nabla^2 M_{xx} = -D\left(\frac{\partial^2 w}{\partial x^2} + \upsilon \frac{\partial^2 w}{\partial y^2}\right) \quad , \quad M_{yy} - (e_0 l_i)^2 \nabla^2 M_{yy} = -D\left(\frac{\partial^2 w}{\partial y^2} + \upsilon \frac{\partial^2 w}{\partial x^2}\right)$$

$$M_{xy} - (e_0 l_i)^2 \nabla^2 M_{xy} = -D(1-\upsilon)\frac{\partial^2 w}{\partial x \partial y} \quad ,$$

(2)

where $e_0 l_i$ and w are nonlocal parameter and transverse displacement, respectively. D is flexural rigidity of the nanoplate and it is defined as [35]

$$D = \frac{Eh^3}{12(1-\upsilon^2)}$$

(3)

We can express stress resultants in terms of lateral deflection on the classical plate theory as follows

$$N_{xx} = N_{yy} = N_r + N_{temp} \quad , \quad N_{xy} = 0$$

(4)

Here, N_r and N_{temp} are the uniform boundary tension and resultant thermal stress respectively and they don't related to x and y directions so all of derivations of boundary tension and resultant thermal stress are zero. For this purpose, the terms $\frac{\partial N_{xx}}{\partial x}$ and $\frac{\partial N_{yy}}{\partial y}$ in Eq. (1) are zero and they are disregarded here. On the basis of the theory of thermal elasticity mechanics, the resultant thermal stress can be written as [35]

$$N_{temp} = \frac{E\alpha}{(1-\upsilon)} h \Delta T$$

(5)

So we have using Eq. (4) and Eq. (2) into Eq. (1) we have the following governing equation of motion in terms of the displacements for the present analysis

$$D\nabla^2\left(\nabla^2 w\right) + \left(N_r + N_{temp}\right)(e_0 l_i)^2 \nabla^2\left(\nabla^2 w\right) - \rho h(e_0 l_i)^2 \nabla^2\left(\frac{\partial^2 w}{\partial t^2}\right) - \left(N_r + N_{temp}\right)\nabla^2 w + \rho h\frac{\partial^2 w}{\partial t^2}$$

$$+ C_d\frac{\partial w}{\partial t} + K_w w - K_G \nabla^2 w - C_d(e_0 l_i)^2 \frac{\partial w}{\partial t} - K_w(e_0 l_i)^2 \nabla^2 w + K_G(e_0 l_i)^2 \nabla^2\left(\nabla^2 w\right) = 0$$

(6)

where ∇^2 is laplacian operator in polar coordinate, the two-dimensional Laplace operator is given by $\nabla^2(\ ) = \partial^2(\ )/\partial r^2 + (1/r)\partial(\ )/\partial r + (1/r^2)\partial^2(\ )/\partial \theta^2$. For free vibration, we can write the motion of the plate in polar coordinates as [37]

$$w(r,\theta,t) = W(r,\theta)e^{i\omega t}$$

(7)

where ω is the natural frequency and $i = \sqrt{-1}$. By inserting Eq.(7) into Eq.(6) yields a four order partial differential equation involving natural mode $W(r,\theta)$

$$\nabla^2\left(\nabla^2 W\right) + \Gamma^2 \nabla^2 W - \Sigma^4 W = 0$$

(8)

where

$$\Gamma^2 = \frac{\left(\rho h \omega^2 (e_0 l_i)^2 \big/ D - \left(N_r + N_{temp}\right)\big/ D - K_G \big/ D - K_W (e_0 l_i)^2 \big/ D - i\omega C_d (e_0 l_i)^2 \big/ D\right)}{\left(1 + \left(N_r + N_{temp}\right)(e_0 l_i)^2 \big/ D + K_G (e_0 l_i)^2 \big/ D\right)} \tag{9}$$

$$\Sigma^4 = \frac{\rho h \omega^2 \big/ D - K_W \big/ D - i\omega C_d \big/ D}{\left(1 + \left(N_r + N_{temp}\right)(e_0 l_i)^2 \big/ D + K_G (e_0 l_i)^2 \big/ D\right)}$$

3   EXACT SOLUTIONS

Using Laplacian operator in polar coordinates, the complete solution to the above equation Eq. (8) can be obtained by superimposing the solutions of the two following Bessel equations

$$\frac{\partial^2 W}{\partial r^2} + \frac{1}{r}\frac{\partial W}{\partial r} + \frac{1}{r^2}\frac{\partial^2 W}{\partial \theta^2} + \frac{\Gamma^2 - \sqrt{\Gamma^4 + 4\Sigma^4}}{2} W = 0 \tag{10}$$

$$\frac{\partial^2 W}{\partial r^2} + \frac{1}{r}\frac{\partial W}{\partial r} + \frac{1}{r^2}\frac{\partial^2 W}{\partial \theta^2} + \frac{\Gamma^2 + \sqrt{\Gamma^4 + 4\Sigma^4}}{2} W = 0 \tag{11}$$

We will put $W(r, \theta) = R(r)\varphi(\theta)$, in the Eq. (10) and (11), afterwards these equations are written by multiplying with $r^2 \big/ R(r)\varphi(\theta)$

$$\frac{r^2}{R(r)}\left(\frac{d^2 R}{dr^2} + \frac{1}{r}\frac{dR}{dr} + \frac{\Gamma^2 - \sqrt{\Gamma^4 + 4\Sigma^4}}{2} R(r)\right) = -\frac{1}{\varphi(\theta)}\frac{d^2\varphi(\theta)}{d\theta^2} \tag{12}$$

$$\frac{r^2}{R(r)}\left(\frac{d^2 R}{dr^2} + \frac{1}{r}\frac{dR}{dr} + \frac{\Gamma^2 + \sqrt{\Gamma^4 + 4\Sigma^4}}{2} R(r)\right) = -\frac{1}{\varphi(\theta)}\frac{d^2\varphi(\theta)}{d\theta^2} \tag{13}$$

Eqs. (12) and (13) are satisfied only if each expression in the above is equal to constant ζ^2. Thus, we obtain three ordinary differential equations as:

$$\frac{d^2\varphi(\theta)}{d\theta^2} + \zeta^2 \varphi(\theta) = 0 \tag{14}$$

$$\frac{d^2 R}{dr^2} + \frac{1}{r}\frac{dR}{dr} + \left(\frac{\Gamma^2 + \sqrt{\Gamma^4 + 4\Sigma^4}}{2} - \frac{\zeta^2}{r^2}\right) R(r) = 0 \tag{15}$$

$$\frac{d^2 R}{dr^2} + \frac{1}{r}\frac{dR}{dr} + \left(\frac{\Gamma^2 - \sqrt{\Gamma^4 + 4\Sigma^4}}{2} - \frac{\zeta^2}{r^2}\right) R(r) = 0 \tag{16}$$

The solution of Eq. (14) will become

$$\varphi(\theta) = A\cos(\zeta\theta) + B\sin(\zeta\theta) \tag{17}$$

Here, *A* and *B* are constants and depend on the boundary conditions. Since $W(r,\theta)$ has to be a continuous function, $\varphi(\theta)$ must be a periodic function with a period of 2π so that $W(r,\theta) = W(r,\theta+2\pi)$. Thus, ζ must be an integer

$$\zeta = m \quad m = 0,1,2,...$$ (18)

Eq. (15) is recognized as forms of Bessel's equation of order $m = \zeta$ with the argument ξr whose solution is given by

$$R_1(r) = A_m^{(1)} J_m(\xi r) + A_m^{(2)} Y_m(\xi r)$$ (19)

J_m, Y_m are Bessel functions of order m of the first and second kind, respectively. The parameter of ξ in the argument of Bessel function is defined as $\xi = \sqrt{\left(\Gamma^2 + \sqrt{\Gamma^4 + 4\Sigma^4}\right)\Big/2}$. Eq. (16) is a Bessel differential equation of order $m = \zeta$ with the argument ηr whose the solution in this case may be written as:

$$R_2(r) = A_m^{(3)} I_m(\eta r) + A_m^{(4)} K_m(\eta r)$$ (20)

where $\eta = \sqrt{\left(-\Gamma^2 + \sqrt{\Gamma^4 + 4\Sigma^4}\right)\Big/2}$ and I_m, K_m are hyperbolic or modified Bessel functions of order m of the first and second kind, respectively. The general solution of Eq. (12) can be expressed as:

$$w(r,\theta) = \begin{pmatrix} A_m^{(1)} J_m(\xi r) + A_m^{(2)} Y_m(\xi r) \\ + A_m^{(3)} I_m(\eta r) + A_m^{(4)} K_m(\eta r) \end{pmatrix} \left(A_m^* \cos(m\theta) + B_m^* \sin(m\theta)\right) \quad m = 0,1,2,...$$ (21)

where the constants $B_m^*, A_m^*, A_m^{(4)}, A_m^{(3)}, A_m^{(2)}, A_m^{(1)}$ and ξ, η depend on the boundary conditions of the nanoplate.

3.1 Clamped boundary condition in outer and inner radius

Let us consider an annular nanoplate as shown in Fig.1, where r is the radius of nanoplate. An annular plate consists of a circular outer boundary and a concentric circular inner boundary. Throughout this work the radius a and b will define the outer and inner boundaries, respectively. We consider an annular graphene sheet with clamped boundary condition on outer and inner edges of the plate. Now, we will substitute the solution Eq. (21) into the clamped boundary conditions at $r = a$ and $r = b$. So, we will have

$$W(r,\theta)\big|_{r=a} = W(r,\theta)\big|_{r=b} = 0$$ (22)

$$\frac{dW(r,\theta)}{dr}\bigg|_{r=a} = \frac{dW(r,\theta)}{dr}\bigg|_{r=b} = 0$$ (23)
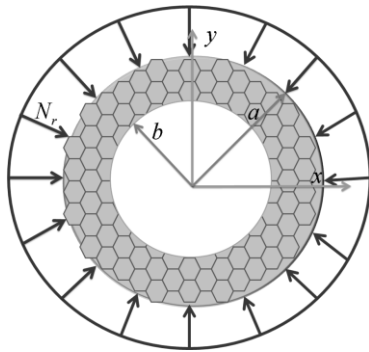
Fig. 1
A continuum plate model of the annular graphene sheet.

This will give four homogeneous equations in four unknowns $A_m^{(1)}, A_m^{(2)}, A_m^{(3)}$ and $A_m^{(4)}$. Similar to the complete circular plates in the previous section for a nontrivial solution, the determinant of coefficient will be zero. The frequency determinant will consist of Bessel function of higher orders.

$$\begin{vmatrix} J_m(\xi a) & Y_m(\xi a) & I_m(\eta a) & K_m(\eta a) \\ J_m'(\xi a) & Y_m'(\xi a) & I_m'(\eta a) & K_m'(\eta a) \\ J_m(\xi b) & Y_m(\xi b) & I_m(\eta b) & K_m(\eta b) \\ J_m'(\xi b) & Y_m'(\xi b) & I_m'(\eta b) & K_m'(\eta b) \end{vmatrix} = 0 \tag{24}$$

3.2 *Simply supported boundary condition in outer and inner radius*

For annular nanoplate with simply supported boundary conditions on outer and inner radius of the plate, the boundary conditions are defined as below

$$W(r,\theta)\big|_{r=a} = W(r,\theta)\big|_{r=b} = 0 \tag{25}$$

$$\left(\frac{\partial^2 W(r,\theta)}{\partial r^2} + \frac{\upsilon}{r} \frac{\partial W(r,\theta)}{\partial r} + \frac{\upsilon}{r^2} \frac{\partial^2 W(r,\theta)}{\partial \theta^2} \right)\Bigg|_{r=a} = 0 \tag{26}$$

$$\left(\frac{\partial^2 W(r,\theta)}{\partial r^2} + \frac{\upsilon}{r} \frac{\partial W(r,\theta)}{\partial r} + \frac{\upsilon}{r^2} \frac{\partial^2 W(r,\theta)}{\partial \theta^2} \right)\Bigg|_{r=b} = 0 \tag{27}$$

By inserting Eq. (21) into Eqs. (25-27), one can write them in the matrix form similar to previous section. To determine nontrivial solutions of the above system of homogeneous equations, it is necessary to equate its determinant to zero. The frequency equation of annular nanoplate with simply supported boundary condition on the outer and inner radius can be written as follows

$$\begin{vmatrix} J_m(\xi a) & Y_m(\xi a) & I_m(\eta a) & K_m(\eta a) \\ C_m^{*(J)} & C_m^{*(Y)} & C_m^{*(I)} & C_m^{*(Y)} \\ J_m(\xi b) & Y_m(\xi b) & I_m(\eta b) & K_m(\eta b) \\ C_m^{**(J)} & C_m^{**(Y)} & C_m^{**(I)} & C_m^{**(K)} \end{vmatrix} = 0 \tag{28}$$

where

$$C_m^{*(\chi)} = \chi''(\xi a) + \frac{\upsilon}{a} \chi'(\xi a) - \frac{m^2 \upsilon}{a^2} \chi(\xi a) \tag{29}$$

$$C_m^{**(\chi)} = \chi''(\xi b) + \frac{\upsilon}{b} \chi'(\xi b) - \frac{m^2 \upsilon}{b^2} \chi(\xi b) \tag{30}$$

Note that the above equations are for $\chi = J$, Y, I, K. For other boundary conditions of annular nanoplate, frequency equations are derived similarly.

The geometric properties of the graphene sheet are denoted by outer radius a, inner radius b, thickness h. For convenience and generality, we introduce the following non-dimensional parameters

$$r = \frac{r^*}{a} \quad , \quad \mu = \frac{e_0 l_i}{a} \quad , \quad \beta = \frac{b}{a} \quad , \quad \overline{K}_W = \frac{K_W a^4}{D} \quad , \quad \overline{K}_G = \frac{K_G a^2}{D} \quad , \quad \overline{C}_d = \frac{C_d a^3 \omega}{D} \quad \overline{N}_r = \frac{N_r a^2}{D} \tag{31}$$

4   NEW VERSION OF DQM FOR ANNULAR NANOPLATE

In this section, for the solution of Eq.(6) the new version DQM [46, 47] is employed. The new version DQM is an efficient numerical method for the solution of partial and ordinary differential equations. Wang and Wang [46] extended the new version of DQM for free vibration analyses of classical sector plates. They presented details formulation of the new version DQM. They showed numerical results indicate that convergence can be achieved with increasing in number of grid points and accurate results could be obtained with 9×9 gird or even higher grid by using the extended DQ method for the cases considered. In this article [46] some other advantages of the new version of DQM technique are also reported. Since DQ technique provides simple formulation and low computational cost, it has been widely used for the analysis of mechanical behaviors of the structural elements at large scale, such as dynamic and stability problems. In recent years, many researchers used DQ approach in solving the governing equations of nanostructures.

Wang et al. [48] employed Timoshenko beam model and DQ method to analyze the vibration behavior of multi-walled carbon nanotubes. Farajpour et al. [19] used DQM for the buckling of orthotropic micro/nanoscale plate under linearly varing in-plane load. In addition, Danesh et al. [10] used DQM for the vibration analysis of tapered nanorod with different boundary conditions. In another work, the nonlocal elastic plate model was developed and applied to the vibration analysis of orthotropic graphene sheets by using DQM [49].

The ordinary DQM is based on a simple mathematical concept that a partial derivative of a function with respect to a space variable at a discrete mesh point (grid point) in domain can be approximated by taking a weighted linear sum of the functional values at all grid points in the whole domain. In the ordinary DQ method, the k-th order derivative of the solution function $w_i^{(k)}$ at grid point i can be computed by [50]

$$w_i^{(k)} = \sum_{j=1}^{N} C_{ij}^{(k)} w_j \qquad (i = 1, 2, ..., N) \tag{32}$$

$C_{ij}^{(k)}$ represents the respective weighting coefficient related to the k-th-order derivative and is obtained as follows:

If $k = 1$, namely, for the first order derivative,

$$C_{ij}^{(1)} = \frac{M^{(1)}(x_i)}{(x_i - x_j) M^{(1)}(x_j)} \qquad for \qquad i \neq j \quad and \quad i, \, j=1,2,...,N \tag{33}$$

For $i = j$ we have

$$C_{ii}^{(1)} = \sum_{j=1(j \neq i)}^{N} C_{ij}^{(1)} \qquad for \qquad i = j \quad and \quad i=1,2,...,N \tag{34}$$

where $M^{(1)}(x)$ is the first order derivative of $M(x)$ and they can be defined as:

$$M(x) = \prod_{j=1}^{N}(x - x_j), \quad M^{(1)}(x_k) = \prod_{j=1,(j\neq k)}^{N}(x_k - x_j) \tag{35}$$

If $k > 1$, the weighting coefficients of the second, third and forth derivatives, may be computed by

$$C_{ij}^{(2)} = \sum_{k=1}^{N}C_{ik}^{(1)}C_{kj}^{(1)}, \; C_{ij}^{(3)} = \sum_{k=1}^{N}C_{ik}^{(1)}C_{kj}^{(2)}, \; C_{ij}^{(4)} = \sum_{k=1}^{N}C_{ik}^{(1)}C_{kj}^{(3)} \qquad i, j=1,2,...,N \tag{36}$$

In the new version DQM, the weighting coefficients of the first and second order derivatives the same as the ordinary DQM are defined. In this method, Wang and Wang [46] considered two degrees of freedom at each end point, w_1, $w_1^{(1)}$ and w_N, $w_N^{(1)}$ in the θ direction but in the r direction only two degrees of freedom, w_N, $w_N^{(1)}$ at points on the outer boundary are defined. Therefore in this method, the third and fourth order derivative in the θ direction are defined by [46]

$$w_i^{(3)} = \sum_{j=1}^{N}\sum_{k=1}^{N}C_{ik}^{(1)}\overset{*}{C}_{kj}^{(2)}w_j + \left(C_{i1}^{(1)}C_{11}^{(1)} + C_{iN}^{(1)}C_{N1}^{(1)}\right)w_1^{(1)} + \left(C_{i1}^{(1)}C_{1N}^{(1)} + C_{iN}^{(1)}C_{NN}^{(1)}\right)w_N^{(1)}$$

$$= \sum_{j=1}^{N}\overset{*}{C}_{ij}^{(3)}w_j + \left(C_{i1}^{(1)}C_{11}^{(1)} + C_{iN}^{(1)}C_{N1}^{(1)}\right)w_1^{(1)} + \left(C_{i1}^{(1)}C_{1N}^{(1)} + C_{iN}^{(1)}C_{NN}^{(1)}\right)w_N^{(1)}$$

$$w_i^{(4)} = \sum_{j=1}^{N}\sum_{k=1}^{N}C_{ik}^{(2)}\overset{*}{C}_{kj}^{(2)}w_j + \left(C_{i1}^{(2)}C_{11}^{(1)} + C_{iN}^{(2)}C_{N1}^{(1)}\right)w_1^{(1)} + \left(C_{i1}^{(2)}C_{1N}^{(1)} + C_{iN}^{(2)}C_{NN}^{(1)}\right)w_N^{(1)} \tag{37}$$

$$= \sum_{j=1}^{N}\overset{*}{C}_{ij}^{(4)}w_j + \left(C_{i1}^{(2)}C_{11}^{(1)} + C_{iN}^{(2)}C_{N1}^{(1)}\right)w_1^{(1)} + \left(C_{i1}^{(2)}C_{1N}^{(1)} + C_{iN}^{(2)}C_{NN}^{(1)}\right)w_N^{(1)}$$

$$(i = 1,2,..., N)$$

where

$$\overset{*}{C}_{1j}^{(2)} = \overset{*}{C}_{1j}^{(2)} \qquad , \quad \overset{*}{C}_{Nj}^{(2)} = \overset{*}{C}_{Nj}^{(2)} \qquad j=1,2,...,N$$

$$\overset{*}{C}_{ij}^{(2)} = C_{ij}^{(2)} \qquad (i=2,3,...,N-1, \; j=1,2,...,N) \tag{38}$$

And the weighting coefficient in the r direction are defined as follow

$$w_i^{(3)} = \sum_{j=1}^{N}\sum_{k=1}^{N}C_{ik}^{(1)}\overset{*}{C}_{kj}^{(2)}w_j + C_{iN}^{(2)}C_{NN}^{(1)}w_N^{(1)} = \sum_{j=1}^{N}\overset{*}{C}_{ij}^{(3)}w_j + C_{iN}^{(1)}C_{NN}^{(1)}w_N^{(1)}$$

$$w_i^{(4)} = \sum_{j=1}^{N}\sum_{k=1}^{N}C_{ik}^{(2)}\overset{*}{C}_{kj}^{(2)}w_j + C_{iN}^{(2)}C_{NN}^{(1)}w_N^{(1)} = \sum_{j=1}^{N}\overset{*}{C}_{ij}^{(4)}w_j + C_{iN}^{(2)}C_{NN}^{(1)}w_N^{(1)} \tag{39}$$

Here

$$\overset{*}{C}_{Nj}^{(2)} = \overset{*}{C}_{Nj}^{(2)} \qquad j=1,2,...,N$$

$$\overset{*}{C}_{ij}^{(2)} = C_{ij}^{(2)} \qquad (i=1,2,3,...,N-1, \; j=1,2,...,N) \tag{40}$$

In terms of new version of DQM, the governing differential equations Eq. (16) at inner grid points for vibration analysis embedded elastic medium and for free vibration analysis of thin circular nanoplates become

$$\left[\begin{array}{l}\left(1+\overline{K}_G\mu^2\right)\left\{\begin{array}{l}\sum_{k=1}^{N}\left(\zeta\overset{*}{C}_{ik}^{(4)}+\frac{2}{\zeta_i}\zeta\overset{*}{C}_{ik}^{(3)}-\frac{1}{\zeta_i^2}\zeta C_{ik}^{(2)}+\frac{1}{\zeta_i^3}\zeta C_{ik}^{(1)}\right)w_{kj}\\[2mm]+\sum_{k=1}^{N}\left(\frac{2}{\zeta_i^2}\zeta C_{ik}^{(2)}-\frac{2}{\zeta_i^3}\zeta C_{ik}^{(1)}\right)\sum_{l=1}^{N}{}^{\theta}C_{jl}^{(2)}w_{kl}\\[2mm]+\sum_{l=1}^{N}\frac{1}{\zeta_i^4}\left(4{}^{\theta}C_{jl}^{(2)}+{}^{\theta}\overset{*}{C}_{jl}^{(4)}\right)w_{il}+\left(\zeta C_{iN}^{(2)}+\frac{2}{\zeta_i}\zeta C_{iN}^{(1)}\right)\zeta C_{NN}^{(1)}\zeta w_{Nj}'\\[2mm]+\frac{1}{\zeta_i^4}\left({}^{\theta}C_{j1}^{(2)}{}^{\theta}C_{11}^{(1)}+{}^{\theta}C_{jN}^{(2)}{}^{\theta}C_{N1}^{(1)}\right){}^{\theta}w_{i1}'+\frac{1}{\zeta_i^4}\left(\begin{array}{l}{}^{\theta}C_{j1}^{(2)}{}^{\theta}C_{1N}^{(1)}+\\{}^{\theta}C_{jN}^{(2)}{}^{\theta}C_{NN}^{(1)}\end{array}\right){}^{\theta}w_{iN}'\end{array}\right\}-\left(\overline{K}_G+\overline{K}_w\mu^2\right)\left\{\begin{array}{l}\sum_{k=1}^{N}\left(\zeta C_{ik}^{(2)}+\frac{1}{\zeta_i}\zeta C_{ik}^{(1)}\right)w_{kj}\\[2mm]+\sum_{l=1}^{N}\frac{1}{\zeta_i^2}{}^{\theta}C_{jl}^{(2)}w_{il}\end{array}\right\}\\[6mm]+\overline{K}_w w_{ij}\end{array}\right]$$

$$+\left[-\overline{C}_d\mu^2\left\{\begin{array}{l}\sum_{k=1}^{N}\left(\zeta C_{ik}^{(2)}+\frac{1}{\zeta_i}\zeta C_{ik}^{(1)}\right)w_{kj}\\[2mm]+\sum_{l=1}^{N}\frac{1}{\zeta_i^2}{}^{\theta}C_{jl}^{(2)}w_{il}\end{array}\right\}+\overline{C}_d w_{ij}\right]=\Omega^2\left[w_{ij}-\mu^2\left[\sum_{k=1}^{N}\left(\zeta C_{ik}^{(2)}+\frac{1}{\zeta_i}\zeta C_{ik}^{(1)}\right)w_{kj}+\sum_{l=1}^{N}\frac{1}{\zeta_i^2}{}^{\theta}C_{jl}^{(2)}w_{il}\right]\right]$$

(41)

where $\zeta = r^*/a$. The ${}^{\zeta}C_{ij}^{(m)}$ is the new version of DQ weighting coefficients of the m-th order derivative in the ζ direction and ${}^{\theta}C_{ij}^{(n)}$ is the new version of DQ weighting coefficients of the n-th order derivative in the θ direction. Eq.(41) can be solved by new version DQM approach for various boundary conditions.

The clamped boundary condition in terms of new version DQM are mathematically represented as:

$$w_{Nj}=0 \qquad \sum_{l=1}^{N}{}^{\zeta}C_{Nl}^{(1)}w_{lj}=0 \qquad\qquad (42)$$

The simply supported boundary condition in terms of new version DQM can be written as:

$$w_{Nj}=0 \qquad \sum_{l=1}^{N}{}^{\zeta}C_{Nl}^{(2)}w_{lj}+\frac{\upsilon}{r_1}\sum_{l=1}^{N}{}^{\zeta}C_{Nl}^{(1)}+\frac{\upsilon}{r_1^2}\sum_{l=1}^{N}{}^{\theta}C_{jl}^{(2)}w_{Nl}+{}^{\zeta}C_{NN}^{(1)}{}^{\zeta}w_{Nj}^{(1)}=0 \qquad (43)$$

The grid point distribution in the ζ and θ direction is [51]

$$\zeta_i=\beta+\frac{(1-\beta)}{2}\left(1-\cos\left(\frac{(i-1)\pi}{(N-1)}\right)\right),\quad i=1,2,...,N \qquad (44)$$

$$\theta_1=0,\quad \theta_i=\frac{2\pi}{2}\left(1-\cos\left(\frac{(2i-3)\pi}{2(N-2)}\right)\right),\quad \theta_N=2\pi \qquad i=2,3,...,\text{ N-1}$$

Using the new version of DQM Eq. (41) can be reduced to an eigenvalue problem as:

$$\left([K]+\omega[C]+\omega^2[M]\right)\begin{Bmatrix}d_b\\d_d\end{Bmatrix}=0 \qquad (45)$$

where the subscript b stands for the elements related to the boundary points while subscript d is associated with the remainder elements. The $[K]$, $[C]$ and $[M]$ are the stiffness, damping and mass matrixes, respectively. For solving the Eq. (39) and reducing it to the standard form of eigenvalue problem, it is convenient to rewrite Eq. (39) as the following first order variable as:

$$\{\dot{Z}\}=[A]\{Z\} \qquad (46)$$

In which the state vector Z and state matrix $[A]$ are defined as:

$$Z = \left\{ \begin{matrix} d_d \\ \dot{d}_d \end{matrix} \right\} \quad and \quad A = \begin{bmatrix} [0] & [I] \\ -\left[M^{-1}K\right] & -\left[M^{-1}C\right] \end{bmatrix} \tag{47}$$

where $[0]$ and $[I]$ are the zero and unitary matrices, respectively. However, the frequencies obtained from the solution of Eq. (41) are complex due to the damping. Hence, the results are containing two real and imaginary parts. The real part is corresponding to the system damping, and the imaginary part representing the system natural frequencies.

5   RESULTS AND DISCUSSION

Effect of temperature on the vibration of annular nanoplate under in-plane pre- load investigated in this paper. We assumed that the scale coefficients are smaller than 2.0 nm because these values for a CNT were taken by Wang and Wang [20]. The properties are considered same as indicated in the reference [33-35]. $E = 1060$ Gpa, $\upsilon = 0.25$, $\rho = 2250 \ kg/m^3$. The temperature dependence of radial and axial coefficient of thermal expansion of SWCNTs is investigated in [40] and concludes that the very tiny thermal expansion coefficient of the tube diameter reflects the strong in-plane C–C bonds in nanotubes. The various values of the thermal expansion coefficients affect the temperature dependence of the observed phonon modes. Also, considerable strain is introduced when nanotubes are mixed with other constituents to form composites for various applications, because of the very different thermal expansion properties of SWNTs and other materials. Moreover, all coefficients vary nonlinearly with temperature and are negative at low or room temperature and become positive at high temperature. Thus, researchers usually use the constant value of $\alpha = -1.6 \times 10^{-6} \ K^{-1}$ for coefficient of thermal expansions at low or room temperatures [20, 33-35 and 42] and use the constant value of $\alpha = 1.1 \times 10^{-6} \ K^{-1}$ for coefficient of thermal expansion at high temperatures. The Winkler and Pasternak coefficients are taken according to [37, 53]. Also, the damping modulus damper is taken according to [43]. These values were used for CNTs [44, 45].

Single layered annular graphene sheets have been considered for the present nonlocal analyses. Following four boundary conditions have been investigated in the vibration analysis of the annular graphene sheets.
SS: Annular graphene sheet with simply supported outer and inner radius.
CS: Annular graphene sheet with clamped outer and simply supported inner radius.
SC: Annular graphene sheet with simply supported outer and clamped inner radius.
CC: Annular graphene sheet with clamped outer and inner radius.

As the results of DQ procedure depend on the number of grid points [46], a convergence test is carried out. The non-dimensional frequencies of circular nanoplate are tabulated in Table 1 for various numbers of grid points and some values of nonlocal parameter. The table is written to obtain the minimum number of grid points required to determine accurate results. The radius of circular nanoplate and aspect ratio are considered 10 nm and 0.5, respectively. Also, the nonlocal parameter 1 nm and low temperature case are considered. It can be easily seen form Table 1 that twelve number of grid points along the r and θ axes is sufficient in order to gain converge solution.

The non-dimensional natural frequency becomes equal zero when the in-plane compressive pre-loads achieve their critical value and the mode of vibration is buckled. We compared the results of annular nanoplates with published data. As shown in Table 2. results of Karamoz and Shahidi [52], compared to results obtained by present work for the critical compressive pre-load of annular nanoplates without thermal change and elastic medium.\

Table 1
Validation and convergence study of new version DQM.

grid point	ΔT (K)											
	SS boundary condition			SC boundary condition			CS boundary condition			CC boundary condition		
	0	50	100	0	50	100	0	50	100	0	50	100
6	31.7124	32.9823	33.7629	43.7624	46.1295	46,2348	44.3795	47.1287	49.6581	70.2341	71.2139	71.2371
8	29.5128	30.2215	31.8325	42.3416	44.9835	44.7692	42.7681	45.8723	49.6581	67.1479	67.2187	69.5481
10	28.1476	29.1810	30.2560	41.8293	42.7368	43.6275	41.9207	43.1294	43.5681	64.7746	66.0981	67.2573
12	28.1476	29.17810	30.2722	41.8293	42.7368	43.6102	41.9207	42.7683	43.5681	64.7746	66.0981	67.2573
14	28.1476	29.1810	30.2722	41.8293	42.7368	43.6102	41.9207	42.7683	43.5681	64.7746	66.0981	67.2573

Table 2
Comparison of results for vibration of the graphene sheet.

Boundary Conditions	References	$e_0 l_i$ (nm)				
		0	0.5	1	1.5	2
SS	Karamoz [52]	41.38	40.89	39.52	38.15	36.76
	Present	41.2546	40.7435	39.3812	38.0190	36.6569
SC	Karamoz [52]	92.25	81.59	70.97	60.34	49.72
	Present	92.1265	81.4818	70.8371	60.1924	49.5478
CS	Karamoz [52]	70.35	63.04	55.73	48.43	41.12
	Present	70.2654	62.8956	55.5258	48.1560	40.8763
CC	Karamoz [52]	159.76	135.07	110.39	85.71	61.02
	Present	159.4326	134.7906	110.1486	85.5066	60.8645

Table 3
Comparison of results for vibration of the annular graphene sheet.

Boundary Conditions	References	$e_0 l_i$ (nm)				
		0	0.5	1	1.5	2
SS	Mohammadi et al. [37]	39.3885	35.9875	28.0736	22.7692	19.5262
	DQ solution	39.4623	36.0087	28.1476	22.8014	19.7246
	Exact solution	39.3885	35.9875	28.0736	22.7692	19.5262
SC	Mohammadi et al. [37]	59.7495	56.3934	41.8278	33.7176	20.4236
	DQ solution	60.0021	56.8926	41.8293	33.9247	20.8971
	Exact solution	59.7495	56.3934	41.8278	33.7176	20.4236
CS	Mohammadi et al. [37]	63.5146	53.7851	41.9183	34.0531	27.7024
	DQ solution	63.9126	54.2005	41.9207	34.0849	27.9461
	Exact solution	63.5146	53.7851	41.9183	34.0531	27.7024
CC	Mohammadi et al. [37]	89.2507	76.5525	64.7592	62.3113	46.7565
	DQ solution	89.7242	76.9142	64.7746	62.5123	46.9214
	Exact solution	89.2507	76.5525	64.7592	62.3113	46.7565

Axisymmetric problem $(m=0)$, here, is considered and outer radius of annular nanoplate is given 20 nm. It can be observed that represented results exactly match with other results reported.

For further validations, the present results are compared to that obtained based on nonlocal elasticity theory for annular nanoplate solutions. We compared the results of annular nanoplates with published data. As shown in Table 3 results of Mohammadi et al. [37], compared to results obtained by present work (Exact solution and DQM results) for the non-dimensional natural frequency of annular nanoplate solutions without in-plane pre-loads and temperature changes. Values of outer radius of annular nanoplate $a=10$ nm and aspect ratio of annular nanoplate $\beta = b/a = 0.5$ have been used in this analysis. It can be observed that represented results exactly match with other results reported. The results of reference [37] are precisely the same with exact solution because the reference [37] solved the free vibration of annular nanoplate by the same method (Bessel function). So, it is normal that the results of two studies (exact solution of this paper and the results of reference [37]) are similar for annular nanoplate without effect of in-plane pre-load and temperature change.

The frequency difference percent is defined as:

$$\text{Difference percent} = \left| \frac{frequency_{\Delta T = T\,(K)} - frequency_{\Delta T = 0}}{frequency_{\Delta T = 0}} \right| \times 100$$

Fig. 2 shows the frequency difference percent with respect to nonlocal parameter. It is seen that the frequency difference percent increases with the increase of the temperature change. Also, the results show that the difference percent increases monotonically by increasing the nonlocal parameter. In other words, that nonlocal solution for difference percent is larger than the local solutions. In Fig.2, the gap between low and high temperature cases increases with increasing the temperature change.
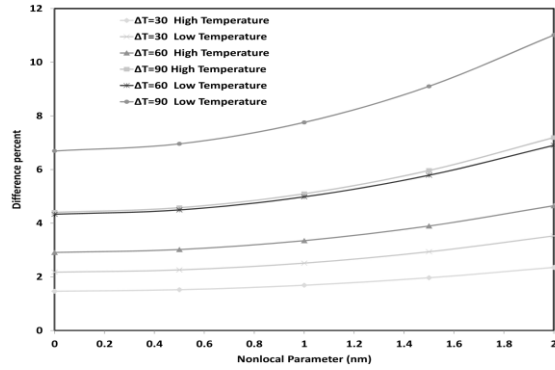
Fig. 2
Variation of difference percent with nonlocal parameter for the cases low and high temperature and various changes temperature.
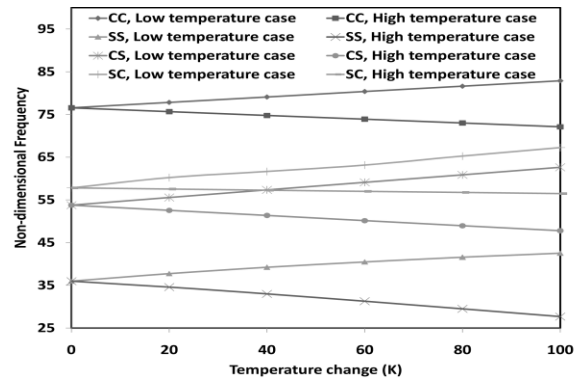

Fig. 3
Change non-dimensional frequency with temperature change for various boundary conditions in the case of low and high temperature.
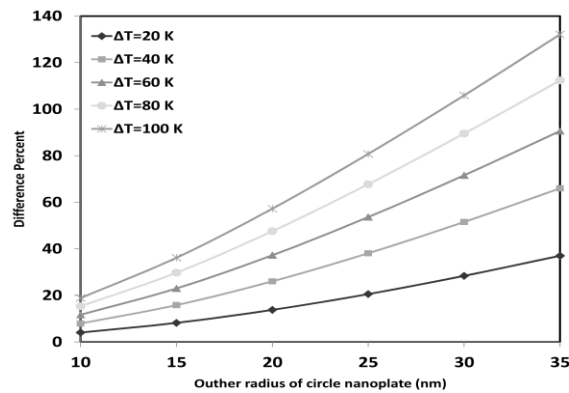

Fig. 4
Change difference percent with radius of circle for various temperature changes.

The relationships between non-dimensional frequency versus temperature change for different boundary condition and low and high temperature case are demonstrated in Fig. 3. From Fig. 3 it is observed that the non-dimensional frequency of the low temperature case is always larger than that of high temperature case. It is demonstrated that the non-dimensional frequency decreases as the change in temperature increases at higher temperature but increases as the change in temperature increases at room or low temperature. Furthermore, the gaps between the two curves (high and low) increases with increasing the temperature change. In other words, the difference between the non-dimensional natural frequencies calculated by high temperature and low temperature decreases with decreasing temperature change. The temperature change is important for graphene sheet with simply supported boundary condition on outer and inner edge, because the slope of curve with simply supported boundary conditions is more than clamped boundary condition curves.

Fig. 4 shows the difference percent versus outer radius of annular nanoplate. It is cleared that the difference percent increases with increase in temperature. It is demonstrated that as the radius of circle increases the difference percent also increases. In other words, at larger radius of circular nanoplate, the effect of temperature change is more important.

Table 4
Change of dimensionless frequency parameters for the four cases different boundary conditions and different temperature change.
$\left(\Omega = \omega a^2 \sqrt{\rho h / D}, \ a = 20 \ nm, \ b/a = 0.5 \ e_0 l_i = 1 \ \text{nm} \right)$

| Boundary Condition	Thermal Case	Temperature Change					
		0	20	40	60	80	100
CC	room or low temperature case	76.5525	77.8325	79.1066	80.3738	81.6336	82.8852
	high temperature case	76.5525	75.6695	74.7852	73.8997	73.0137	72.1283
SS	room or low temperature case	35.9875	37.7473	39.2251	40.4844	41.5775	42.5442
	high temperature case	35.9875	34.5823	33.0095	31.2912	29.4905	27.7019
CS	room or low temperature case	53.7851	55.5609	57.34	59.115	60.8793	62.6257
	high temperature case	53.7851	52.5694	51.3603	50.1594	48.9681	47.7875
SC	room or low temperature case	57.814	58.233	58.678	59.1565	59.6778	60.2523
	high temperature case	57.814	57.5377	57.2685	57.006	56.7471	56.4914
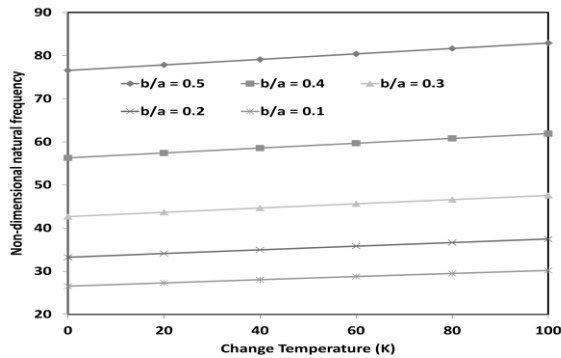
Fig. 5
Change non-dimensional natural frequency with change temperature for various aspect ratios.

Table 4. presents the change of the frequency parameters with temperature change for the annular nanoplates with $\upsilon = 0.3$. To illustrate the effect of boundary condition and thermal case on frequency response, in this section we tabulate the lowest six temperature change for different thermal case and four cases different boundary conditions of annular nanoplate. In this investigation, we consider the non-dimensional frequency of first mode number, the outer radius of the annular nanoplate 20 nm and the nonlocal parameter is 1 nm. From this table it is seen that frequency parameters increase with increase of temperature change for all boundary condition and room or low temperature case. In the other hand, it is observed that the effects of the temperature change on the non-dimensional frequency are different for the case of low and high temperature. This table shows the important influence of temperature change, in the cases low and high temperature case on the non-dimensional frequency of annular graphene sheet.

To illustrate the effect of aspect ratio on the non-dimensional frequency, in this section, the non-dimensional frequency versus temperature change of annular nanoplate for different aspect ratio is plotted in Fig. 5.

Fig. 5 shows the important influence of aspect ratio on the natural frequency of annular graphene sheet with CC boundary conditions and low temperature case. The radius of circular nanoplate r=10 nm and nonlocal parameter $e_0 l_i$=1 nm are considered. It is found that the non-dimensional frequency increases with increase of aspect ratio from 0.1 to 0.5 and temperature change in low temperature case. Similarly, these phenomena are observed for annular nanoplate with different boundary conditions.

The effect of temperature change on the frequency of annular graphene sheet embedded in an elastic medium is studied. The dimensionless Winkler constant $\bar{K}_W$, for the surrounding polymer matrix is taken in the range of 0–400, dimensionless shear modulus $\bar{K}_G$ is varied in the range 0-10 [53]. Similar values of modulus parameter were also applied by Liew et al [54]. Also, the dimensionless damping modulus is taken in the range of 0-200 [43, 44]. The relationships between frequency difference percent versus dimensionless Winkler constant $\bar{K}_W$, dimensionless shear modulus $\bar{K}_G$ and the dimensionless damping modulus $\bar{C}_d$ for different temperature changes and low and high temperature case are demonstrated in Figs. 6 (a), (b) and (c) . A scale coefficient $\left(e_0 l_i = 2.0 \right)$ nm is used in the analysis. As can be seen, the Winkler constant or shear modulus decreases then the effect of temperature on the difference percent increases. It can be seen that the difference percent increases with increasing the temperature change. For larger temperature change, the decline of difference percent is quite important. Also, the difference

percent for low temperature case is larger than that for case of high temperature. Furthermore, the decline for the high temperature case is much less than that for case of low temperature. These plots show the important influence of temperature change, in the cases low and high temperature case on the non-dimensional frequency of embedded graphene sheet. In Figs. 6(a), (b) and (c) the gap between low and high temperature cases increases with increasing the temperature change.

In Fig. 7, the plot of non-dimensional natural frequency with respect to outer radius of annular nanoplate is demonstrated. All of pre-loads in this paper are dimensionless and are introduced in Eq.(31). These results are plotted here for the annular nanoplate under non-dimensional compressive pre-load, the case of annular nanoplate without in-plane pre-load and different values of nonlocal parameter. The clamped boundary condition and first mode number is considered. From Fig. 7 it is observed that decreasing the nonlocal parameter yields to increase the natural frequency. This indicates that increasing the nonlocal parameter leads to decrease in the stiffness of body. Furthermore, the non-dimensional natural frequency increases the radius of the nanoplate increases. It is clear as a matter of fact that, the influence of nonlocal effect reduces by increasing of radius. Furthermore, with further increase of radius the curves become smooth in nature. Approximately, at $a \geq 50$ nm all results converge to the classical frequencies $(e_0 l_i = 0)$. This insinuates that the nonlocal effect decreases with growth of the plate radius and disappears after a certain radius. This may be explained that the wave length gets larger by decreasing of radius which increases the effect of the small scale parameter. Moreover, the non-dimensional natural frequency for annular nanoplate with in-plane pre-load is smaller than that without in-plane pre-load. The influence of nonlocal parameter is larger for annular nanoplate with in-plane pre-load in comparison with annular nanoplate without in-plane pre-load. Further, at annular nanoplate with in-plane pre-load all results converge to the local frequency $(e_0 l_i = 0)$ at higher radiuses. It is seen that influence of nonlocal effect is higher for annular nanoplate with in-plane pre-loads.
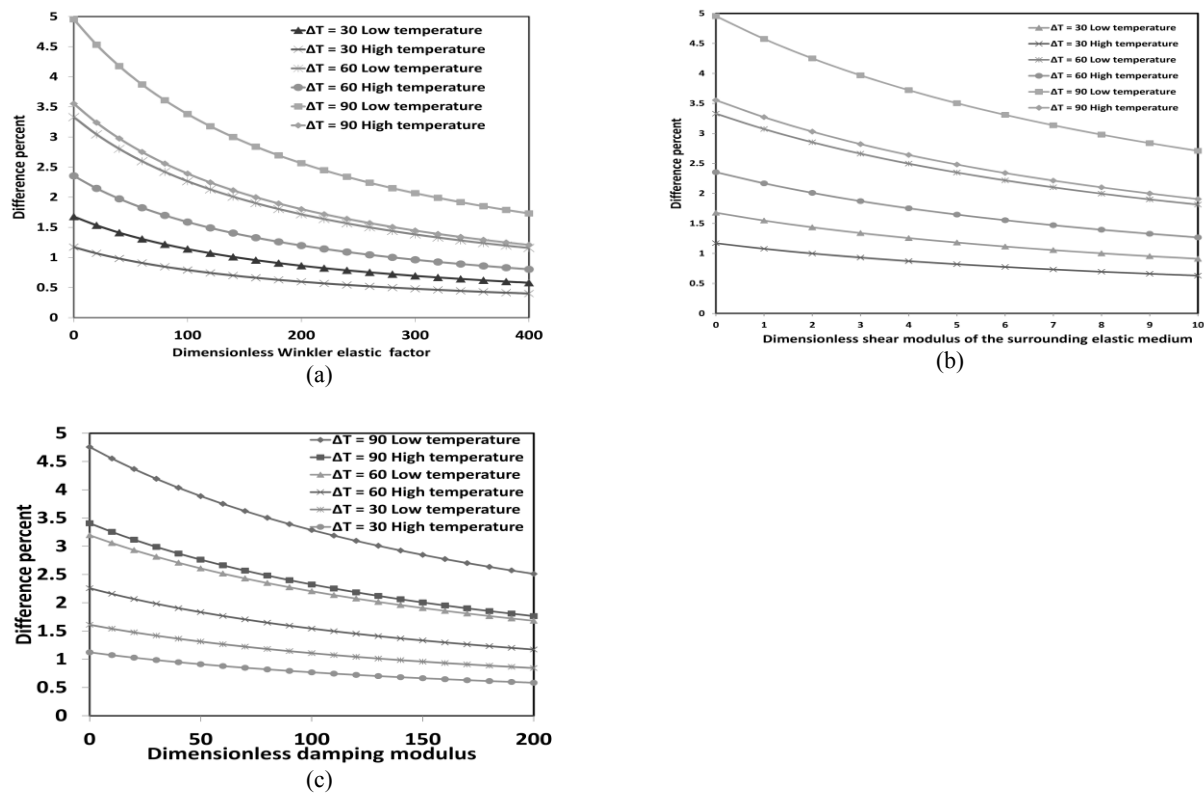

Fig.6
Change difference percent frequency of circular nanoplate versus a) dimensionless Winkler elastic factor, b) dimensionless shear elastic factor, c) dimensionless damping modulus for low and high temperature case and various temperature changes.
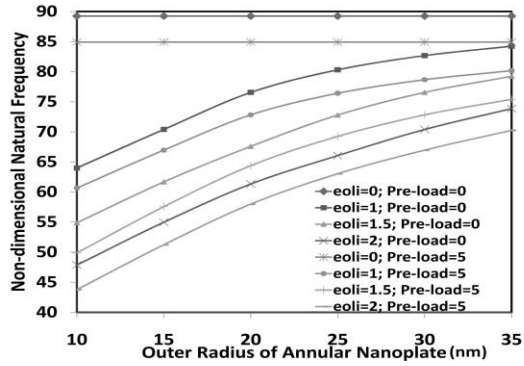
Fig. 7
Variation of non dimensional frequency with outer radius of an annular graphene sheet for various nonlocal parameters with non-dimensional in-plane pre-load and without in-plane pre-load.

Fig.8 shows the comparison of the non-dimensional frequency parameters for four boundary conditions of annular nanoplates. To illustrate the effect of boundary condition on frequency response, in this section we plot the non-dimensional natural frequency parameters for different nonlocal parameters and four cases different boundary conditions of annular nanoplate. Here, the outer radius of annular nanoplate and aspect ratio are 10 nm and 0.5 respectively. From this figure it is seen that frequency parameters increase with decrease of nonlocal parameter for all boundary conditions. As seen from Fig. 8, the small scale effect also depends on the boundary conditions. As the boundary conditions became flexible, the small scale effect kept on decreasing. The small scale effect for SS case is much less than that for CC case. Furthermore, effects of small scale on the frequency of the annular nanoplate for CC, CS, SC and SS boundary conditions are in decreasing order. Therefore, in the vibration analyses it is needful to include the nonlocal elasticity theory for stiffer boundary conditions.

We introduce a term 'frequency shift percent' (FSP) for the present study. Frequency shift percent is defined as:

$$frequency \text{ shift percent} = \frac{\Omega_{with \text{ elastic medium}} - \Omega_{without \text{ elastic medium}}}{\Omega_{without \text{ elastic medium}}} \times 100$$

Variation of frequency shift percent with nonlocal parameter is shown for first mode of vibration Fig.9. The non-dimensional parameter of elastic medium such as shear modulus parameter $\overline{K}_G$, Winkler modulus parameter $\overline{K}_W$ and damping modulus of damper $\overline{C}_d$ for the surrounding polymer matrix is gotten 10, 400 and 100 respectively. The value of damping modulus damper was applied by Ghorbanpour arani et al. [43, 44]. The curves show that the frequency shifts are sensitive to the modulus of the surrounding elastic medium. Also, the frequency shift of shear and spring mediums are maximum and minimum, respectively and visco-Pasternak case located between. As can be seen, the frequency shift increases by increasing the elastic foundation stiffness and decrease as nonlocal parameter.
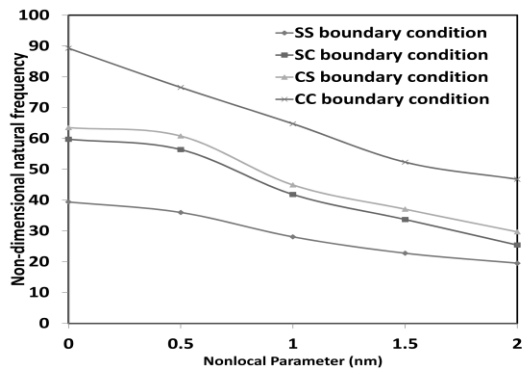

Fig. 8
Change of dimensionless frequency parameters for the four cases different boundary conditions and nonlocal parameter.
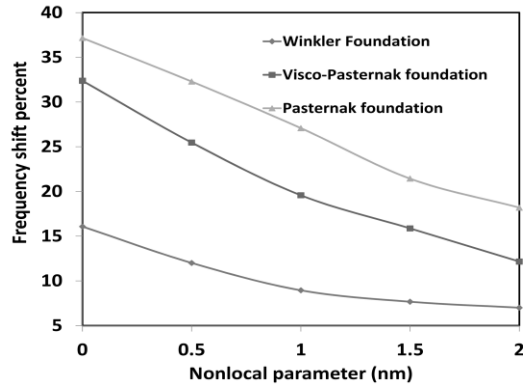
Fig. 9
Effect of elastic medium on the frequency shift percent for different nonlocal parameter.

6   CONCLUSIONS

This study illustrates the significance of small scale effects on the vibration behavior of SLGSs under in-plane pre-stressed via nonlocal continuum mechanics. The closed form solutions for the free vibration nanoscale annular nanoplates are obtained. Results for annular graphene sheets with simply supported and clamped edges are presented. From the results, the following conclusions are noticeable:

- By increasing in-plane tensile pre-stress the natural frequencies increases and the higher in-plane compressive pre-stress leads to lower natural frequencies.
- In the case of compressive in-plane pre-stressed the frequency fraction will increase with the radius of nanoplate increasing and in-plane pre-stressed.
- At smaller radius of annular nanoplate, the effect of in-plane pre-stressed is more important.
- By increasing radius, the influence of nonlocal effect reduces.
- The influence of nonlocal effect is higher for annular nanoplate with in-plane pre-stressed.
- The non-dimensional natural frequency decreases at high temperature case with increasing the temperature change.
- The effect of temperature change on the non-dimensional frequency vibration becomes the opposite at low temperature case in comparison with the high temperature case.
- The nonlocal effect also depends on the temperature change. The influence of nonlocal effect for higher temperature case is much more than that for room temperature case.
- The effect of nonlocal parameter increases with increasing the temperature change.
- The difference percent increases monotonically by increasing the nonlocal parameter.
- The difference between low and high temperature cases increases with increasing the temperature change.
- The effect of temperature on the frequency vibration increases with increasing the radius of annular nanoplate.
- The effects of small length scale and surrounding elastic medium are significant to the mechanical behavior of nanoplates or SLGSs and cannot be ignored.

ACKNOWLEDGMENTS

REFERENCES

[1]   Sorop T.G., Jongh L.J., 2007, Size-dependent anisotropic diamagnetic screening in superconducting nanowires, *Physical Review B* **75**: 014510-014515.

[2]   Iijima S., 1991, Helical microtubules of graphitic carbon, *Nature* **354**: 56–58.

[3]   Kong X.Y, Ding Y, Yang R, Wang Z.L., 2004, Single-crystal nanorings formed by epitaxial self-coiling of polar nanobelts, *Science* **303**:1348-1351.

[4]   Wong E.W., Sheehan P.E., Lieber C.M., 1997, Nanobeam mechanics:elasticity, strength and toughness of nanorods and nanotubes, *Science* **277**:1971–1975.

[5]   Zhou S.J., Li Z.Q., 2001, Metabolic response of platynota stultana pupae during and after extended exposure to elevated CO2 and reduced O2 atmospheres, *Journal of insect physiology* **31**:401-409.

[6]   Fleck N.A., Hutchinson J.W., 1997, Strain gradient plasticity, *Applied Mechanics* **33**:295–361.

[7]   Yang F., Chong A.C.M., Lam D.C.C., Tong P., 2002, Couple stress based strain gradient theory for elasticity, *International Journal of Solids Structure* **39**:2731-2743.

[8]   Eringen A.C., 1983, On differential equations of nonlocal elasticity and solutions of screw dislocation and surface waves, *Journal Applied Physics* **54**:4703-4711.

[9]   Farajpour A., Danesh M., Mohammadi M., 2011, Buckling analysis of variable thickness nanoplates using nonlocal continuum mechanics, *Physica E* **44**:719–727.

[10]   Danesh M., Farajpour A., Mohammadi M., 2012, Axial vibration analysis of a tapered nanorod based on nonlocal elasticity theory and differential quadrature method, *Mechanics Research Communications* **39**:23-27.

[11]   Aydogdu M., 2009, Axial vibration of the nanorods with the nonlocal continuum rod model, *Physica E* **41**:861-864.

[12]   Babaei H., Shahidi A. R., 2010, Small-scale effects on the buckling of quadrilateral nanoplates based on nonlocal elasticity theory using the Galerkin method, *Archive Applied Mechanics* **81**:1051–1062.

[13]   Lu P., Lee H.P., Lu C., Zhang P.Q., 2006, Dynamic properties of flexural beams using a nonlocal elasticity model, *Journal Applied Physics* **99**:073510.

[14]   Duan W. H., Wang C. M., 2007, Exact solutions for axisymmetric bending of micro/nanoscale circular plates based on nonlocal plate theory, *Nanotechnology* **18**:385704.

[15]   Mohammadi M., Moradi A., Ghayour M., Farajpour A., 2014, Exact solution for thermo-mechanical vibration of orthotropic mono-layer graphene sheet embedded in an elastic medium, *Latin American Journal of Solids and Structures* **11**(3): 437-458.

[16]   Mohammadi M., Farajpour A., Goodarzi M., Dinari F., 2014, Thermo-mechanical vibration analysis of annular and circular graphene sheet embedded in an elastic medium, *Latin American Journal of Solids and Structures* **11** (4): 659-683.

[17]   Mohammadi M., Goodarzi M., Ghayour M. Farajpour A., 2013, Influence of in-plane pre-load on the vibration frequency of circular graphene sheet via nonlocal continuum theory, *Composites Part B* **51**:121-129.

[18]   Mohammadi M. , Farajpour A. , Goodarzi M. , Shehni nezhad pour H., 2014, Numerical study of the effect of shear in-plane load on the vibration analysis of graphene sheet embedded in an elastic medium, *Computational Materials Science* **82**: 510-520.

[19]   Farajpour A., Shahidi A. R., Mohammadi M., Mahzoon M., 2012, Buckling of orthotropic micro/nanoscale plates under linearly varying in-plane load via nonlocal continuum mechanics, *Composite Structures* **94**:1605-1615.

[20]   Wang Q., Wang C.M., 2007, The constitutive relation and small scale parameter of nonlocal continuum mechanics for modelling carbon nanotubes, *Nanotechnology* **18**(7):075702.

[21]   Mohammadi M., Farajpour A., Goodarzi M., Heydarshenas R., 2013, Levy type solution for nonlocal thermo-mechanical vibration of orthotropic mono-layer graphene sheet embedded in an elastic medium, *Journal of Solid Mechanics* **5** (2): 116-132.

[22]   Moosavi H., Mohammadi M., Farajpour A., Shahidi S. H., 2011, Vibration analysis of nanorings using nonlocal continuum mechanics and shear deformable ring theory, *Physica E* **44**:135-140.

[23]   Mohammadi M., Goodarzi M., Ghayour M., Alivand S., 2012, Small scale effect on the vibration of orthotropic plates embedded in an elastic medium and under biaxial in-plane pre-load via nonlocal elasticity theory, *Journal of Solid Mechanics* **4**(2):128-143.

[24]   Ke L. L., Yang J., Kitipornchahi S., Bradford M. A., Wang Y. S., 2013, Axisymmetric nonlinear free vibration of size-dependent functionally graded annular microplates, *Composites: Part B* **53**:207-217.

[25]   Rahmat Talabi M., Saidi A. R., 2013, An explicit exact analytical approach for free vibration of circular/annular functionally graded plates bonded to piezoelectric actuator/sensor layers based on Reddy's plate theory, *Applied Mathematical Modelling* **37**:7664-7684.

[26]   Mohammadi M., Farajpour A., Moradi M., Ghayour M., 2013, Shear buckling of orthotropic rectangular graphene sheet embedded in an elastic medium in thermal environment, *Composites Part B* **56**:629-637.

[27]   Civalek Ö., Akgöz B., 2013, Vibration analysis of micro-scaled sector shaped graphene surrounded by an elastic matrix, *Computational Materials Science* **77**:295-303.

[28]   Murmu T., Pradhan S.C., 2009, Vibration analysis of nano-single-layered graphene sheets embedded in elastic medium based on nonlocal elasticity theory, *Journal Applied Physics* **105**:064319-064327.

[29]   Pradhan S.C., Phadikar J.K., 2009, Small scale effect on vibration of embedded multi layered graphene sheets based on nonlocal continuum models, *Physics Letters A* **373**:1062–1069.

[30]   Wang Y.Z., Li F.M., Kishimoto K., 2011, Thermal effects on vibration properties of doublelayered nanoplates at small scales, *Composites Part B: Engineering* **42**:1311-1317.

[31]   Reddy C.D., Rajendran S., Liew K.M., 2006, Equilibrium configuration and continuum elastic properties of finite sized graphene, *Nanotechnology* **17**:864 -870.

[32]   Aksencer T., Aydogdu M., 2011, Levy type solution method for vibration and buckling of nanoplates using nonlocal elasticity theory, *Physica E* **43**:954 -959.

[33]   Malekzadeh P., Setoodeh A.R., Alibeygi Beni A., 2011, Small scale effect on the thermal buckling of orthotropic arbitrary straight-sided quadrilateral nanoplates embedded in an elastic medium, *Composite Structures* **93**:2083–2089.

[34]   Satish N., Narender S., Gopalakrishnan S., 2012, Thermal vibration analysis of orthotropic nanoplates based on nonlocal continuum mechanics, *Physica E* **44**:1950 -1962.

[35]   Prasanna Kumar T.J., Narendar S., Gopalakrishnan S., 2013, Thermal vibration analysis of monolayer graphene embedded in elastic medium based on nonlocal continuum mechanics, *Composite Structures* **100**:332-342.

[36]   Farajpour A., Mohammadi M., Shahidi A.R., Mahzoon M., 2011, Axisymmetric buckling of the circular graphene sheets with the nonlocal continuum plate model, *Physica E* **43**:1820-1825.

[37]   Mohammadi M., Ghayour M., Farajpour A., 2013, Free transverse vibration analysis of circular and annular graphene sheets with various boundary conditions using the nonlocal continuum plate model, *Composites Part B* **45**:32-42.

[38]   Paul A., Tipler G. M., 2008, *Physics for Scientists and Engineers*, Worth Publishers, New York.

[39]   Murray B.W., O'mara I., William C., Robert B., Lee P., 1990, *Handbook of Semiconductor Silicon Technology*, Park Ridge, New Jersey, Noyes Publications.

[40]   Jiang H., Liu R., Huang Y., Hwang K.C., 2004, Thermal expansion of single wall carbon nanotube, *Journal of Engineering of Material and Technology* **126** (3):265-270.

[41]   Alamusi Hu N., Jia B., Arai M., Yan C., Li J., Liu Y., Atobe S., Fukunaga H., 2012, Prediction of thermal expansion properties of carbon nanotubes using molecular dynamics simulations, *Computational Materials Science* **54**:249-254.

[42]   Yao X., Han Q., 2006, Buckling analysis of multiwalled carbon nanotubes under torsional load coupling with temperature change, *Journal of Engineering Materials and Technology* **128**:419-427.

[43]   Ghorbanpour Arani A., Shiravand A., Rahi M., Kolahchi M., 2012, Nonlocal vibration of coupled DLGS systems embedded on visco-pasternak foundation, *Physica B* **407**:4123-4131.

[44]   Ghorbanpour Arani A., Roudbari M. A., 2013, Nonlocal piezoelastic surface effect on the vibration of visco-Pasternak coupled boron nitride nanotube system under a moving nanoparticle, *Thin Solid Films* **542**:232-241.

[45]   Ghorbanpour Arani A., Roudbari M. A., Amir S., 2012, Nonlocal vibration of SWBNNT embedded in bundle of CNTs under a moving nanoparticle, *Physica B* **407**:3646-3653.

[46]   Wang X., Wang Y., 2004, Free vibration analyses of thin sector plates by the new version of differential quadrature method, *Computer Methods in Applied Mechanics and Engineering* **193**:3957-3971.

[47]   Mohammadi M., Ghayour M., Farajpour A., 2011, Analysis of free vibration sector plate based on elastic medium by using new version of differential quadrature method, *Journal of Solid Mechanics in Engineering* **3**(2) :47-56.

[48]   Wang C.M., Tan V.B.C, Zhang Y.Y., 2006, Timoshenko beam model for vibration analysis of multi-walled carbon nanotubes, *Journal of Sound and Vibration* **294**:1060-1072.

[49]   Pradhan S. C., Kumar A., 2011, Vibration analysis of orthotropic graphene sheets using nonlocal elasticity theory and differential quadrature method., *Composite Structures* **93**:774 -779.

[50]   Shu C., 2000, *Differential Quadrature and Its Application in Engineering*, Great Britain Springer.

[51]   Wang X., Wang Y., 2004, Re-analysis of free vibration of annular plates by the new version of differential quadrature method, *Journal of Sound and Vibration* **278**:685-689.

[52]   Karamooz Ravari M.R., Shahidi A.R., 2012, Axisymmetric buckling of the circular annular nanoplates using finite difference method, *Meccanica* **47**:1-10.

[53]   Murmu T., Pradhan S.C., 2009, Buckling analysis of a single-walled carbon nanotube embedded in an elastic medium based on nonlocal elastici ty and Timoshe nko beam theory and using DQM, *Physica E* **41**:1232 -1239.

[54]   Liew K. M., He X. Q., Kitipornchai S., 2006, Predicting nanovibration of multi-layered graphene sheets embedded in an elastic matrix, *Acta Material* **54**:4229-4236.